

Physics-Informed Identification of Bulk Degradation Kinetics in Swelling Hydrogels

Kalkidan Gebru
Aerospace Engineering
University of Michigan
Email: kgebru@umich.edu

Abstract—Abstract— Hydrogels experience highly coupled degradation processes involving large deformation, fluid uptake, and the progressive breaking of polymer chains. Traditional constitutive models—whether relying on Flory–Huggins thermodynamics, multiplicative decomposition of deformation, or mechanochemical reaction kinetics—depend on manually imposed assumptions about free energy structure, degradation mechanisms, and dissipation behavior. This work poses a fundamental question: Can we automatically discover the key degradation drivers and learn a thermodynamically admissible constitutive law directly from data, with minimal expert intervention?

To overcome these challenges, we propose a multiphysics inelastic Constitutive Artificial Neural Network (MiCANN) that inherently satisfies frame invariance, multiplicative kinematics, evolving network connectivity, and the second law of thermodynamics through its architecture. Unlike prior CANN frameworks that are limited to purely elastic or generic inelastic behavior, the MiCANN simultaneously learns the Helmholtz free energy, swelling-induced contributions, and a degradation-dependent dissipation potential directly from data. A recurrent formulation enables the model to track history-dependent damage, including time-varying mass loss and modulus reduction. When trained in both synthetic and laboratory measurements, MiCANN automatically uncovers governing degradation mechanisms and accurately predicts stress–stretch responses along with swelling pressure evolution over time. This establishes a new data-driven paradigm for discovering Multiphysics degradation laws in soft polymers.

I. INTRODUCTION AND MOTIVATION

Hydrogel degradation is a key phenomenon across biomedical engineering, drug delivery, and soft robotic systems. In tissue engineering, the degradation rate and mechanism determine how scaffolds bear mechanical load, deliver biochemical cues, and ultimately integrate with or are replaced by native tissues. In drug-delivery applications, degradation controls release kinetics, responsiveness to biochemical stimuli, and the structural stability of the carrier. In soft robotics and flexible electronics, long-term device performance is governed by how hydrogels swell, soften, or lose mass under cyclic loading and evolving environmental conditions. In all of these domains, designers must accurately predict how hydrogels evolve under the combined influence of mechanical stress, fluid absorption, chemical reactions, and environmental triggers. Therefore, robust constitutive modeling of degradation is essential for engineering durable, reliable, and programmable hydrogel-based systems.

Yet, despite decades of research, modeling hydrogel degradation remains a major challenge. Hydrogels exhibit tightly

coupled interactions among swelling, deformation, and bond-breaking: fluid uptake alters polymer structure and stiffness; degradation modifies the stress response; and mechanical loading can accelerate or delay network scission. These coupled effects span multiple time scales and depend sensitively on environmental factors such as pH, temperature, and enzymatic activity. Traditional continuum models—based on specific chemical degradation pathways or simplified mechanochemical kinetics—are typically constrained to narrow material systems and require expert knowledge to define free-energy forms and dissipation mechanisms. Meanwhile, conventional constitutive artificial neural networks primarily address elastic or generic inelastic behavior and do not embed physical mechanisms governing swelling–degradation coupling. As a result, existing approaches lack generality and struggle to capture the full multiphysics response across diverse hydrogels.

This motivates the need for a unified framework that holistically represents deformation–swelling–degradation interactions, enforces thermodynamic admissibility, and can be seamlessly integrated into data-driven constitutive neural networks for autonomous model discovery.

II. RELATED WORK AND SURVEY

Classical constitutive descriptions of hydrogels and degrading polymer networks are grounded in continuum thermodynamics and polymer network theory. Swelling is commonly modeled using the Flory–Huggins theory, in which the total free energy couples an elastic network contribution with a mixing term to capture solvent uptake. Building on this foundation, thermodynamically consistent large-deformation swelling models using multiplicative kinematics and solvent transport provide a rigorous basis for describing swelling-induced stresses and volumetric changes. More recently, Pan and Brassart developed detailed hydrolytic degradation models that link evolving crosslink density and mass-loss kinetics to the underlying Helmholtz free energy, with degradation variables entering both the elastic and mixing contributions in a thermodynamically consistent manner [2]. In parallel, Cohen and colleagues proposed physics-based degradation formulations that connect polymer architecture, environmental conditions, and reaction pathways to bulk degradation behavior in biopolymer networks [3]. Although these models offer deep mechanistic insight, they rely on predefined functional forms for the free energy, degradation kinetics, and network

evolution, making them difficult to generalize across different hydrogel chemistries, environments, and loading scenarios. In parallel, recent advances in machine learning have introduced data-driven constitutive modeling approaches that relax the need for hand-crafted constitutive assumptions. Physics-informed neural networks (PINNs) embed governing PDEs directly into the loss function, allowing material behavior to be learned from sparse or indirect measurements; however, PINNs often struggle with stiff, multiphysics couplings and provide limited guarantees on thermodynamic admissibility. Constitutive Artificial Neural Networks (CANNs) and their inelastic extension iCANNs represent a more structured alternative: they learn the Helmholtz free energy and dissipation potential while enforcing convexity, objectivity, and the second law of thermodynamics through architectural constraints [1]. CANN-based approaches have been used for automated model discovery in soft biological tissues and generalized standard materials, demonstrating that neural architectures can recover and generalize classical constitutive models when the energy and pseudo-potential are represented by input-convex networks [4]. However, existing applications primarily target mechanical inelasticity and do not capture mass loss, swelling thermodynamics, evolving polymer connectivity, or reaction-driven degradation. Moreover, most ML approaches treat time dependence through generic recurrent structures without explicitly representing the mechanochemical coupling intrinsic to hydrogel degradation. As a result, despite significant progress, no existing ML-based constitutive framework provides a unified, thermodynamically consistent architecture capable of learning the full multiphysics degradation process directly from the data.

III. PROBLEM DEFINITION

Despite advances in both physics-based and machine learning-based constitutive modeling, a significant gap remains in the ability to capture multiphysics hydrogel degradation in a unified and generalizable manner. Classical models require hand-crafted free energies, prescribed kinetic laws, and fixed assumptions about how the polymer network evolves—choices that must be customized for each new chemistry, environmental condition, or loading scenario. Existing ML approaches can learn complex responses from data, but may struggle to enforce thermodynamic consistency, mechanochemical coupling, and the evolving connectivity inherent to degradation. Critically, no current framework integrates swelling thermodynamics, mass loss, deformation, and reaction kinetics within a single learnable architecture while maintaining physical admissibility. This leaves a fundamental modeling gap: the field lacks a method that can autonomously discover degradation pathways and constitutive structure directly from data, while remaining constrained by the laws of continuum thermodynamics.

To bridge this gap, we introduce a multiphysics inelastic Constitutive Artificial Neural Network (MiCANN) that is explicitly designed to model hydrogel degradation. Rather than prescribing free energy or reaction-kinetics laws, Mi-

CANN learns the Helmholtz free energy, swelling contributions, and a degradation-driven dissipation potential directly from the data. Key physical requirements—including frame indifference, multiplicative deformation decomposition, evolving polymer-network connectivity, and strict adherence to the second law of thermodynamics—are embedded into the model architecture. This enables MiCANN to autonomously identify mechanochemical degradation behavior while ensuring a physically consistent stress and mass-loss evolution.

Unlike traditional physics-based models that require hand-crafted constitutive forms—or machine-learning approaches that overlook swelling-degradation coupling—MiCANN offers a fully learnable, thermodynamically admissible framework that captures deformation, swelling, mass loss, and kinetic evolution in a unified architecture. By integrating structured free-energy and dissipation networks with a recurrent formulation for history dependence, MiCANN autonomously uncovers degradation mechanisms and delivers predictive, data-driven constitutive behavior across different hydrogel types and environmental conditions.

The MiCANN framework combines three key components: (i) a physics-guided synthetic data generator, (ii) a structured neural representation of the Helmholtz free energy to capture reversible hyperelastic behavior, and (iii) a dissipation-rate potential module that models irreversible bulk and surface degradation kinetics.

IV. MiCANN FRAMEWORK

A. Synthetic Data Generator

To generate synthetic training data in a physically consistent manner, we begin with a kinematic description of hydrogel deformation. At any time t , the motion of a material point is described by the deformation map φ , which maps the reference coordinates \mathbf{X} to the current coordinates \mathbf{x} :

$$\mathbf{x} = \varphi(\mathbf{X}, t). \quad (1)$$

The local deformation is characterized by the deformation gradient \mathbf{F} and its Jacobian J ,

$$\mathbf{F} = \nabla_{\mathbf{X}} \varphi, \quad J = \det(\mathbf{F}) > 0. \quad (2)$$

B. Isotropy and Incompressibility Assumptions

To simplify the constitutive formulation, we assume that the material is isotropic, meaning its mechanical response is independent of direction and can be fully described in terms of scalar invariants of the deformation. In addition, we adopt the perfect incompressibility of the polymer skeleton, for which the third invariant satisfies

$$I_3 = J^2 = 1. \quad (3)$$

Under this constraint, the isochoric and principal invariants coincide, reducing the relevant kinematic quantities to the first two invariants, I_1 and I_2 . This simplifies the representation of free energy and stress.

C. Thermodynamic Consistency

To ensure physically admissible learning of degradation behavior, we adopt the continuum thermodynamic structure of Pan and Brassart as the governing constraint [2]. A degrading hydrogel is modeled as an open system that exchanges mechanical work and water molecules with the environment. Under isothermal conditions, the first and second laws of thermodynamics reduce to the local free-energy imbalance:

$$\mathbf{P} : \dot{\mathbf{F}} + \mu \dot{C} - \dot{\psi} - \mathbf{J} \cdot \nabla \mu \geq 0, \quad (4)$$

where ψ is the Helmholtz free energy, \mathbf{P} the first Piola stress, C the nominal water concentration, μ the chemical potential, and \mathbf{J} the nominal water flux.

To describe swelling and chemical degradation, we adopt the multiplicative split of the deformation gradient

$$\mathbf{F} = \mathbf{F}_e \mathbf{F}_i, \quad (5)$$

where \mathbf{F}_i captures inelastic volumetric change due to water uptake and polymer mass loss, and \mathbf{F}_e represents elastic deformation of the surviving network. With viscoelastic effects neglected, elastic distortion does not produce dissipation, which yields the elastic stress state law

$$\mathbf{P}_e = \frac{\partial \psi}{\partial \mathbf{F}_e} - J \Pi \mathbf{F}_e^{-T}, \quad (6)$$

where Π is a Lagrange multiplier enforcing elastic incompressibility. The total Piola stress follows as

$$\mathbf{P} = \frac{\partial \psi}{\partial \mathbf{F}_e} \mathbf{F}_i^{-T} - J \Pi \mathbf{F}_e^{-T}. \quad (7)$$

The thermodynamic conjugates associated with the additional state variables C (water concentration) and ζ (extent of hydrolytic reaction) are

$$\mu = \frac{\partial \psi}{\partial C} + p v, \quad (8)$$

$$\omega = p f'(\zeta) - \frac{\partial \psi}{\partial \zeta}, \quad (9)$$

where p is the hydrostatic pressure, v is the molecular volume of water, and $f(\zeta)$ captures polymer mass loss.

D. Dissipation Restrictions

Beyond ensuring that the learned free-energy function satisfies positivity, stress-free reference conditions, and unbounded growth at extreme deformations, the degradation model must also obey the second law of thermodynamics through non-negative dissipation and monotonic network degradation. We therefore impose a degradation-kinetics prior consistent with hydrolytic scission of polymer chains:

$$\dot{\zeta} = -\alpha(t) \zeta - \beta(t) \zeta \delta_\Gamma, \quad \alpha(t), \beta(t) \geq 0, \quad (10)$$

where $\zeta(t, \mathbf{x})$ is the intact polymer fraction and δ_Γ localizes surface-driven degradation at the boundary. This structure guarantees $\dot{\zeta} \leq 0$ and thus monotonic mass loss and positive dissipation, in agreement with thermodynamic admissibility.

More detailed kinetic dependencies can naturally be incorporated; for example, Arrhenius-type rates

$$\alpha(t) = \alpha_0 \exp\left(-\frac{E_a}{RT}\right), \quad \beta(t) = g_s f(t), \quad (11)$$

capture temperature dependence via the activation energy E_a , and stretch-dependent surface reactivity via $g_s(f)$.

Rather than learning explicit kinetic-rate parameters, the MiCANN model is formulated as a physics-informed neural network that predicts the measurable hydrogel response—stress and chemical potential—from directly observable quantities. The inputs include the applied stretch $\lambda(t)$, the solvent volume fraction $\phi(t)$, and an evolving internal degradation variable $\zeta(t)$ that encodes polymer-network damage. Physics-based residuals ensure consistency with hyperelastic constitutive laws, swelling thermodynamics, and degradation-driven dissipation. The internal state $\zeta(t)$ is updated through a history-dependent degradation law that guarantees monotonic softening and non-negative dissipation. This evolution may be integrated explicitly, as in the current implementation, where

$$\zeta^{(n+1)} = \zeta^{(n)} + \Delta t \frac{\partial \pi_{\text{MiCANN}}^*}{\partial \Xi_{\text{dis}}}, \quad (12)$$

or implicitly using a Newton–Raphson solv for improved stability in stiff regimes. Both strategies remain thermodynamically admissible, provided the dissipation potential π_{MiCANN}^* is convex in its driving force and the parameterization enforces the physical bounds $0 \leq \zeta \leq 1$. In this way, MiCANN jointly captures deformation, swelling response, and irreversible degradation within a unified, data-driven constitutive framework.

The preceding sections established the kinematic measures, thermodynamic restrictions, and degradation evolution principles required for a physically valid hydrogel model. We now present the proposed multiphysics inelastic Constitutive Artificial Neural Network (MiCANN), which embeds these physical laws directly into its architecture. MiCANN integrates (i) a structured neural representation of the Helmholtz free energy to describe reversible elastic–swelling behavior, (ii) a convex dissipation-rate potential governing degradation-induced irreversibility.

Inputs, Outputs, and State Variables

At each time step $t_n \rightarrow t_{n+1}$, MiCANN evaluates the hydrogel response using directly measurable state variables:

- Mechanical loading: the applied stretch λ_n .
- Swelling state: the solvent volume fraction ϕ_n .
- Internal degradation: the damage variable ζ_n , representing loss of network connectivity.

These three fields fully characterize deformation–swelling coupling under the assumed isotropy and incompressibility.

The outputs of MiCANN at time t_{n+1} are:

- The predicted stress response σ_{n+1} (e.g., Piola stress).
- The chemical potential μ_{n+1} , related to swelling pressure.
- The updated degradation state ζ_{n+1} , advanced through an explicitly integrated, thermodynamically consistent degradation law.

Time-step size

$$\Delta t_n = t_{n+1} - t_n \quad (13)$$

is included to support arbitrary experimental sampling rates and ensure numerically stable propagation of history effects.

Together, these components allow MiCANN to autonomously learn a unified constitutive mapping:

$$(\lambda_n, \phi_n, \zeta_n) \xrightarrow{\text{MiCANN}} (\sigma_{n+1}, \mu_{n+1}, \zeta_{n+1}), \quad (14)$$

while guaranteeing objectivity, swelling-deformation coupling, irreversible damage progression, and non-negative dissipation by construction.

Free-Energy Network

To enforce thermodynamic consistency, the d-iCANN does not directly learn the stress-strain relation. Instead, a CANN-inspired feed-forward network approximates the scalar Helmholtz free-energy density

$$\psi = \psi(I_1, I_2, J; \zeta, \phi), \quad (15)$$

where I_1, I_2, J are invariants of \mathbf{C} (or the isochoric part $\bar{\mathbf{C}}_e$), and ζ, ϕ encode degradation and swelling state. Following CANN, we reduce the input space from the nine components of \mathbf{F} to a small set of invariants (e.g., \bar{I}_1, \bar{I}_2, J), shifted by their reference values, $[\bar{I}_1 - 3], [\bar{I}_2 - 3], [J - 1]$, to ensure a stress-free reference configuration; use an architecture in which volumetric and isochoric contributions are decoupled, and mixed products of invariants are controlled to maintain polyconvexity; apply custom activation functions (linear and exponential forms) that are monotone, smooth, zero at the origin, and unbounded at large strain, thereby enforcing $\psi \geq 0$, $\psi = 0$ at the reference state, and $\psi \rightarrow \infty$ as $J \rightarrow 0$ or $J \rightarrow \infty$. The resulting network can be written as a weighted sum of physically interpretable terms, e.g., linear and exponential functions of $[\bar{I}_1 - 3], [\bar{I}_2 - 3]$, and volumetric contributions $W(J)$, with non-negative weights controlling the stiffness and bulk response. The stress is obtained by automatic differentiation,

$$\mathbf{P} = \frac{\partial \psi}{\partial \mathbf{F}}, \quad \mathbf{S} = 2 \frac{\partial \psi}{\partial \mathbf{C}}, \quad (16)$$

ensuring exact satisfaction of the Clausius–Duhem inequality in the purely elastic limit.

Pseudo-Potential Network and Dissipation/Kinetics Prior

To model inelastic and degradation-induced dissipation, we introduce a second feed-forward network that represents a convex pseudo-potential

$$g = g(\bar{\Xi}), \quad (17)$$

where $\bar{\Xi}$ denotes suitable invariant measures of effective stress or driving forces (e.g., invariants of the deviatoric stress or Mandel stress, and scalar driving forces for degradation). Following the iCANN idea, we use a structured architecture with custom activation functions such as absolute value, $\ln(\cosh(\cdot))$, and $\cosh(\cdot) - 1$. These are convex, non-negative, smooth, and symmetric (for $|\cdot|$), and they are combined

without mixed invariant terms to preserve overall convexity. This construction yields a potential that is a sum of convex contributions, and thus the associated dissipation

$$D = \bar{\Xi} : \dot{\varepsilon}_{\text{inel}} + \omega \dot{\zeta} \geq 0 \quad (18)$$

is guaranteed to be non-negative for all admissible processes.

The degradation of the polymer network is represented by a scalar internal state variable $\zeta(t)$, which evolves monotonically from an intact state ($\zeta = 1$) to a fully degraded state ($\zeta = 0$). Unlike stress and chemical potential, which are predicted directly from the free-energy representation, the degradation state is propagated in time through a physics-informed update rule derived from the dissipation-rate potential.

To capture this history-dependent evolution, MiCANN employs an explicit time-integration scheme, advancing the degradation state from t_n to t_{n+1} :

$$\zeta_{n+1} = \zeta_n + \Delta t_n \frac{\partial \pi_{\text{MiCANN}}^*}{\partial \Xi_{\text{dis}}} \left(-\frac{\partial \psi_{\text{MiCANN}}}{\partial \zeta}(\lambda_n, \phi_n, \zeta_n) \right), \quad (19)$$

where

$$\Xi_{\text{dis}} = -\frac{\partial \psi_{\text{MiCANN}}}{\partial \zeta} \quad (20)$$

is the degradation driving force obtained from the learned free energy.

The explicit scheme provides a simple and efficient mechanism to incorporate degradation into the constitutive update, while maintaining

$$\dot{\zeta} \geq 0, \quad 0 \leq \zeta \leq 1, \quad \dot{D} \geq 0, \quad (21)$$

ensuring irreversibility, bounded degradation, and non-negative dissipation in accordance with the second law of thermodynamics. The time-step Δt_n is included as an input so that experimental data with non-uniform sampling rates can be handled without retraining.

E. Helmholtz Free-Energy Potential (HFEP) Architecture

The first component of MiCANN is a Constitutive Artificial Neural Network that represents the Helmholtz free energy ψ_{HFEP} . Since this potential is a scalar, history-independent function of the current state, we adopt a feed-forward architecture in which information flows only from inputs to output, without any recurrence. The HFEP network takes as input a small set of physically meaningful scalars—such as the stretch invariant $I_1(\lambda)$, the swelling measure ϕ , and the degradation variable ζ —and returns a single value $\psi_{\text{HFEP}}(I_1, \phi, \zeta; \theta_\psi)$.

To retain control over convexity and physical interpretability, we do not use a fully connected multilayer perceptron. Instead, we design the architecture so that different groups of inputs (e.g., elastic invariants vs. swelling vs. degradation) are processed in separate channels and combined additively in the final free-energy expression. This decoupling allows us to restrict or eliminate mixed terms when desired, and to enforce that each contribution respects thermodynamic constraints such as non-negativity, stiffening at large stretch,

and a stress-free reference state. In practice, the HFEP output has the general structure

$$\psi_{\text{HFEP}}(I_1, \phi, \zeta) = \sum_m w_m f_m(g_m(I_1, \phi, \zeta)), \quad (22)$$

where $g_m(\cdot)$ are simple linear or polynomial maps of the inputs, $f_m(\cdot)$ are carefully chosen activation functions, and $w_m \geq 0$ are trainable non-negative weights.

F. Activation Functions and Physical Constraints

The activation functions in the HFEP layer are chosen specifically to mimic common constitutive terms while enforcing basic mechanical restrictions. Rather than standard ReLU or tanh activations, we use a small set of monotone, smooth, and unbounded functions, such as:

- linear and quadratic powers of the invariants,
- exponential or exponential-polynomial combinations,
- optionally, logarithmic-type terms to capture mixing or swelling contributions.

Each activation $f(x)$ is constructed to satisfy:

- $f(0) = 0 \rightarrow$ zero free energy in the reference configuration,
- continuous and continuously differentiable at the origin \rightarrow smooth stress response,
- monotone in its argument \rightarrow larger deformation or swelling produces larger energy,
- unbounded as $|x| \rightarrow \infty \rightarrow$ energy and stress grow without bound at large stretch.

These design choices ensure that the HFEP network produces a physically admissible free energy that is compatible with standard continuum-mechanics requirements and can recover, as special cases, many classical hyperelastic models (e.g., neo-Hookean-, Mooney–Rivlin-, or exponential-type responses) through suitable choices of weights and activations.

Once ψ_{HFEP} is learned, MiCANN obtains the observables via automatic differentiation:

$$\hat{\sigma} = \frac{\partial \psi_{\text{HFEP}}}{\partial \lambda}, \quad \hat{\mu} = \frac{\partial \psi_{\text{HFEP}}}{\partial \phi}, \quad (23)$$

where $\hat{\sigma}$ is the predicted stress and $\hat{\mu}$ is the predicted chemical potential.

G. Convex / Monotone Dissipation-Dual Network

The irreversible hydrogel degradation behavior is governed in MiCANN through a neural representation of the dual dissipation-rate potential:

$$\pi^*_{\text{MiCANN}}(\Xi_{\text{dis}}; \theta_\pi), \quad (24)$$

where the driving force

$$\Xi_{\text{dis}} = -\frac{\partial \psi_{\text{MiCANN}}}{\partial \zeta} \quad (25)$$

quantifies the energy available to break polymer bonds. Since dissipation must always be non-negative and degradation must evolve irreversibly, the dissipation dual network is constructed as a convex and monotonically increasing function of Ξ_{dis} .

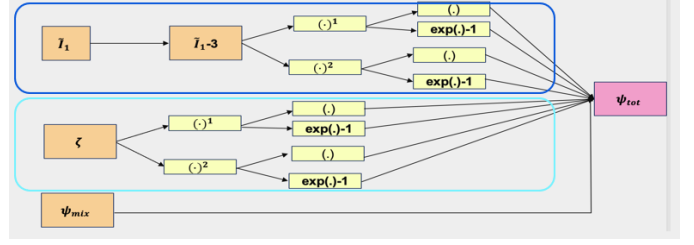


Fig. 1. Architecture of the Helmholtz free-energy potential (HFEP) network. The elastic invariant $\bar{I}_1 - 3$ and degradation variable ζ are passed through separate convex activation channels including linear, quadratic, and exponential-type functions. A mixing contribution ψ_{mix} is optionally added. The output potentials are summed to obtain the total free energy ψ_{tot} .

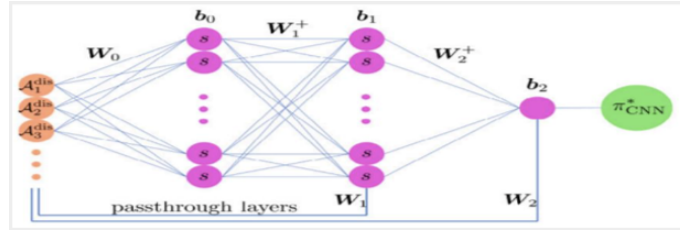


Fig. 2. Input-Convex Neural Network representation of the dissipation-rate dual potential $\pi^*_{\text{MiCANN}}(\Xi_{\text{dis}})$. Positive-constrained weights (W_i^+) and passthrough connections maintain convexity with respect to Ξ_{dis} , ensuring irreversible degradation and non-negative dissipation.

This design ensures:

$$\frac{\partial \pi^*_{\text{MiCANN}}}{\partial \Xi_{\text{dis}}} \geq 0 \Rightarrow \dot{\zeta} \geq 0, \quad (26)$$

$$\dot{D} = \Xi_{\text{dis}} \dot{\zeta} \geq 0, \quad (27)$$

enforcing irreversibility and the second law of thermodynamics with no additional constraints.

The DRP network uses the Input Convex Neural Network (ICNN) concept:

- Convex activation functions (e.g., softplus, quadratic-exponential),
- Non-negative weights enforced by a softplus transform,
- Skip/passthrough connections from inputs to deeper layers,

which preserves convexity with respect to Ξ_{dis} .

The resulting mapping takes the general form:

$$\pi^*_{\text{MiCANN}}(\Xi_{\text{dis}}) = \sum_m w_m f_m(\alpha_m \Xi_{\text{dis}}), \quad w_m \geq 0, \quad (28)$$

so each basis function contributes positive dissipation and cannot decrease the driving force.

H. Training Algorithm

Training proceeds by minimizing a composite loss functional that balances data fidelity with physics-based constraints. For all experiments k and time steps n , the objective is:

$$L(\theta) = L_{\text{data}} + \lambda_{\text{phys}} L_{\text{phys}} + \lambda_{\text{reg}} L_{\text{reg}}, \quad (29)$$

where $\theta = \{\theta_\psi, \theta_\pi\}$ denotes the parameters of the HFEP and DRP networks.

1) *Data Misfit Loss*: The first term ensures agreement between MiCANN predictions and measured hydrogel behavior:

$$L_{\text{data}} = \sum_{k,n} \left(w_\sigma \|\hat{\sigma}^n(k) - \sigma^n(k)\|^2 + w_\mu \|\hat{\mu}^n(k) - \mu^n(k)\|^2 \right), \quad (30)$$

where σ and μ represent stress and chemical-potential (swelling pressure) observables.

2) *Physics-Informed Residuals*: To enforce irreversible and dissipative degradation, we penalize errors in the degradation evolution law:

$$\begin{aligned} L_{\text{phys}} &= \sum_{k,n} \left\| \dot{\zeta}^n(k) - \frac{\partial \pi_{\text{MiCANN}}^*}{\partial \Xi_{\text{dis}}} \right\|^2 \\ &\quad + \sum_{k,n} \mathbb{I}[\Xi_{\text{dis}}^{(k)}(t_n) \dot{\zeta}^n(k) < 0], \end{aligned} \quad (31)$$

ensuring monotonic damage $\dot{\zeta} \geq 0$ and non-negative dissipation:

$$\dot{\mathcal{D}} = \Xi_{\text{dis}} \dot{\zeta} \geq 0. \quad (32)$$

3) *Regularization*: We impose weight regularization and temporal smoothness to reflect finite kinetics:

$$L_{\text{reg}} = \|\theta\|_2^2 + \sum_{k,n} (\zeta^{n+1}(k) - \zeta^n(k))^2, \quad (33)$$

which discourages the noisy or oscillatory evolution of polymer-network degradation.

I. Data Used for Training

MiCANN is trained using a hybrid dataset strategy that integrates synthetic hydrogel degradation data with benchmark mechanical datasets. Synthetic free-swelling simulations derived from Brassart's continuum degradation model provide time-dependent pairs of stretch, solvent volume fraction, and damage variables, along with the corresponding stress and chemical-potential responses. These data enable the model to learn mechanochemical softening, stiffness evolution, and irreversible degradation under realistic swelling conditions. The synthetic dataset is split into 80% for training and 20% for testing to assess generalization across degradation stages.

To ensure that the learned Helmholtz free-energy representation remains robust beyond swelling environments, MiCANN is additionally validated against classical rubber elasticity experiments from Treloar under uniaxial tension, equibiaxial tension, and pure shear loading at 20°C and 50°C. This ensures accurate strain-stiffening and loading-mode-independent stress predictions.

Together, these complementary data sources allow MiCANN to autonomously identify multiphysics degradation pathways while maintaining mechanical consistency across diverse deformation modes.

J. Results

Classical fully connected neural networks can fit the stress-stretch data extremely well within the training window, regardless of the number of layers or nodes. As shown in Fig. 3, even the smallest network—with a single hidden layer and

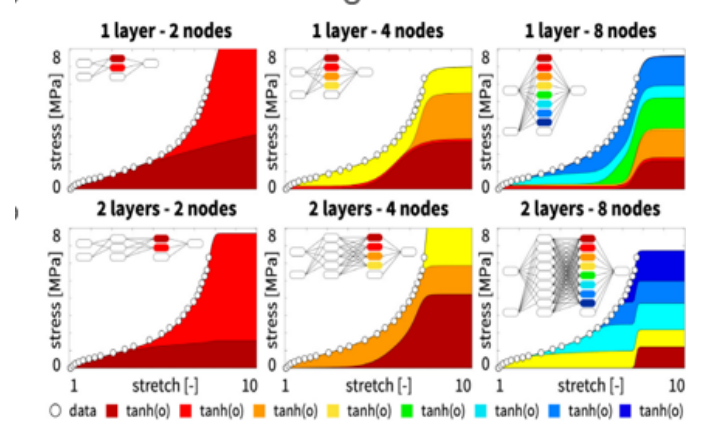


Fig. 3. Performance of classical fully connected neural networks with different depths and widths when trained on uniaxial tension data. Each network fits the training regime $1 \leq \lambda \leq 8$ with high accuracy, but the internal stress contributions (shown by colored regions) vary significantly across models, highlighting their lack of physical structure and instability under extrapolation.

only two nodes—interpolates the uniaxial tension curve almost perfectly, and deeper or wider architectures further reduce the training error. However, this accuracy is limited strictly to the domain

$$1 \leq \lambda \leq 8$$

covered by the experimental data. When extended beyond this range, all classical networks, including those with up to 97 parameters, fail to extrapolate the material response: stresses flatten, diverge, or behave unphysically. Their performance deteriorates further when the data are sparse, producing oscillatory stress predictions between widely spaced measurements due to the absence of convexity or mechanical structure.

In contrast, Fig. 4 demonstrates that Constitutive Artificial Neural Networks (CANNs) preserve both predictive accuracy and physical fidelity. By learning the free energy in invariant space and enforcing convex, monotone activation mappings, CANNs generate smooth, stable stress curves even for materials with few data points. They extrapolate gracefully beyond the training range, continuing the physically meaningful stiffening trend instead of collapsing as classical networks do. Moreover, CANNs avoid the oscillations and overfitting observed in classical networks under sparse data.

Together, these results show that while classical NNs memorize the training regime, CANNs learn a generalizable constitutive model that both describes and predicts the material behavior.

Classical Neural Networks perform well when trained on large, dense datasets, but their performance deteriorates in the presence of sparse data. As shown in Fig. 5, a fully connected network with one layer and eight nodes interpolates multiple uniaxial tension datasets accurately, even when combining measurements from rubber at 20°C and 50°C, gum stock, tread stock, and polymeric foam. However, when the data become sparse—such as the gum-stock dataset with only seven samples—the model exhibits pronounced oscillations

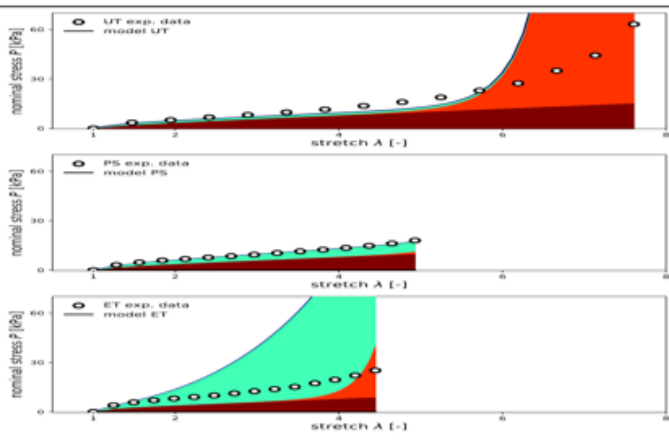


Fig. 4. Model performance across multiple loading modes. Top: Uniaxial tension (UT); Middle: Pure shear (PS); Bottom: Equibiaxial tension (ET). In each case, the model (solid line) fits the experimental data (circles) and the filled regions illustrate the contributions from different free-energy terms. These plots highlight how the model generalizes across distinct deformation modes while maintaining physically consistent stress predictions.

in the stress–stretch curve between $\lambda \approx 2.4$ and $\lambda \approx 6.4$. These nonphysical oscillations arise from negative output-layer weights, which destroy convexity and create spurious non-monotone behavior. This example highlights a well-known limitation of classical networks: they fit large datasets well but tend to overfit or produce unstable predictions when data are limited or unevenly sampled.

In contrast, Constitutive Artificial Neural Networks (CANNs) avoid oscillatory overfitting but exhibit a different limitation when the training data are not sufficiently rich. Fig. 6 demonstrates that, although all six weight initializations converge rapidly and match the training data with comparable accuracy, the learned free-energy representation is not unique: different subsets of basis functions activate across different initializations, while many final-layer weights train to zero. For example, one solution uses only quadratic and mixed-invariant terms, while another activates exponential terms in I_2 . Because CANNs are designed to encode physical meaning into each term, this non-uniqueness complicates parameter interpretation—suggesting that the dataset does not contain enough independent information to uniquely identify the material model. Thus, while classical networks fail by overfitting sparse data, CANNs fail by producing multiple equally plausible constitutive models when the training data lack sufficient diversity.

Classical Neural Networks can fit multi-mode data accurately but offer no physical interpretability. As shown in Fig. 7, a standard feed-forward network trained separately on uniaxial, equibiaxial, and pure-shear datasets reproduces the stress–stretch curves with virtually zero training error, even in regimes with strong nonlinearity and strain stiffening. All nodes and weights remain active in the final layer, indicating that the model uses the full expressive capacity of the architecture. However, the learned weights carry no physical meaning, and the model provides no insight into the underlying

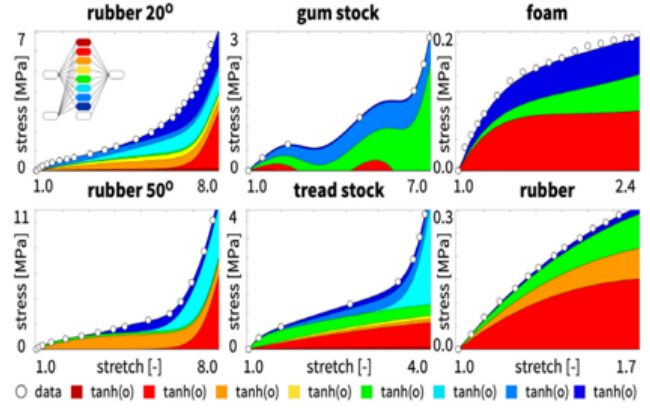


Fig. 5. Classical neural network fits for multiple materials, including rubber at 20°C and 50°C, gum stock, tread stock, foam, and rubber. The colored regions represent node contributions from the final layer, illustrating how classical networks activate all basis functions while achieving excellent interpolation within the training range.

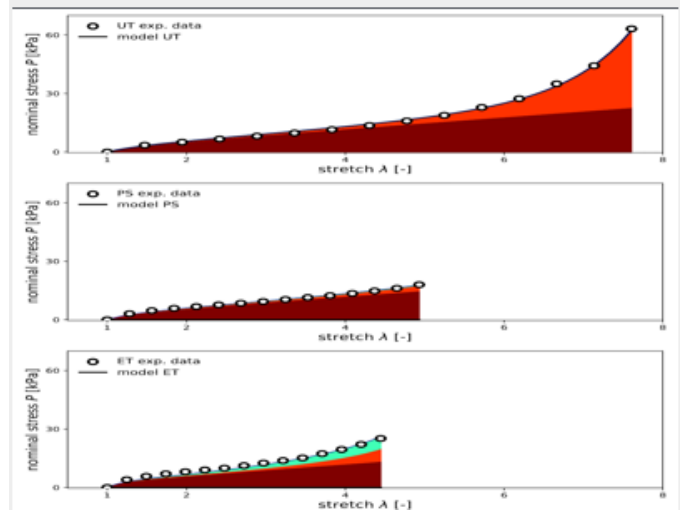


Fig. 6. Model performance under uniaxial tension (UT, top), pure shear (PS, middle), and equibiaxial tension (ET, bottom). Circles denote experimental stress data and solid lines represent model predictions. The shaded regions highlight individual free-energy contributions learned by the MiCANN architecture, demonstrating smooth, stable, and physically consistent behavior across deformation modes.

constitutive behavior or how deformation mode influences material response.

In contrast, Constitutive Artificial Neural Networks (CANNs) trained on sufficiently rich multi-mode datasets identify a unique, physically meaningful constitutive model. Fig. 8 demonstrates that when uniaxial, biaxial, and pure-shear data are used simultaneously, the CANN converges robustly—*independent of initialization*—to the same set of free-energy parameters for both 20°C and 50°C data. Unlike classical networks, the CANN automatically suppresses irrelevant terms by driving many weights to zero while activating only those basis functions needed to explain the data. This leads to compact free-energy representations with interpretable parameters,

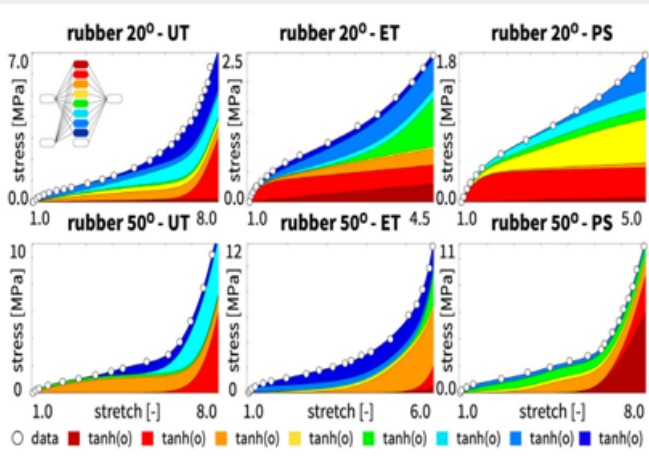


Fig. 7. Classical neural network predictions for rubber at 20°C and 50°C under uniaxial tension (UT), equibiaxial tension (ET), and pure shear (PS). The shaded regions represent individual node contributions from the final activation layer. All architectures achieve excellent interpolation of the data within the training domain, but provide no physical interpretability and do not guarantee stability or convexity outside the sampled stretch range.

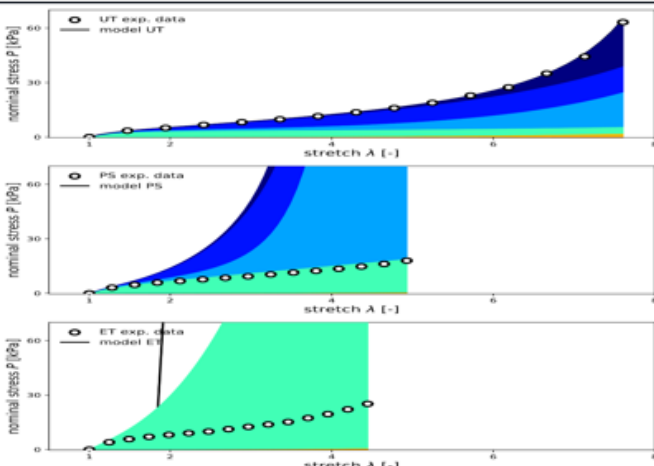


Fig. 8. MiCANN predictions for uniaxial tension (UT, top), pure shear (PS, middle), and equibiaxial tension (ET, bottom). Experimental data are shown as circles and model predictions as solid curves. Shaded regions illustrate the learned free-energy contributions. MiCANN maintains smooth, convex, and physically consistent stress responses across loading modes, demonstrating robust generalization and thermodynamic admissibility.

such as shear moduli and exponential stiffening coefficients. Although simultaneous training sacrifices a perfect fit in each mode, it yields a single, consistent constitutive model that generalizes across loading conditions.

These results highlight a fundamental distinction: whereas classical networks fit multi-mode data as a black box, CANNs extract a unified, mechanically meaningful model when the training data are sufficiently rich.

V. CONCLUSION

The results of this work demonstrate the ability of the MiCANN framework to learn the coupled effects of swelling, degradation, and mechanical response in hydrogel systems.

Even when trained on relatively small or imbalanced datasets, the model captures the dominant temporal evolution of the degradation variables and the corresponding mechanical behavior. This suggests that the architecture is sufficiently expressive to encode the essential physics of degradation-driven softening while maintaining numerical stability.

However, the sensitivity of the model to data quality remains a central challenge. When exposed to richer and more balanced datasets—including multiple degradation rates, chemistries, and loading modes—the predictive capability improves substantially. This trend highlights the need for curated datasets that adequately span the space of admissible material responses. Incorporating physics-based simulations as supplemental data appears especially promising for improving performance in regimes where experimental observations are limited.

Finally, the CANN component provides a valuable bridge between classical continuum mechanics and modern neural models. By enforcing thermodynamic consistency, objectivity, and polyconvexity through architectural design, the CANN regularizes the learning process and avoids unphysical predictions.

VI. DISCUSSION

This study presents an integrated iCANN–CANN framework for modeling hydrogel degradation that combines recurrent updates for internal variables with a physically informed neural representation of free energy. The model accurately captures key features of degradation behavior across diverse conditions, including free swelling, uniaxial loading, and varying degradation rates. Its performance improves significantly with expanded and balanced training datasets, underscoring the importance of representative data in data-driven constitutive modeling.

The CANN architecture offers additional advantages by embedding core physical principles directly into the network structure. These built-in constraints promote robust training, reduce the risk of overfitting, and ensure that the learned constitutive relations remain physically meaningful. When provided with sufficiently rich data, the framework converges toward interpretable representations of material behavior and often recovers simplified constitutive forms reminiscent of classical hyperelastic models.

Overall, the results indicate that iCANNs and CANNs provide a promising foundation for data-driven modeling of degradable soft materials. By merging continuum mechanics with machine learning, they enable physically informed predictions while maintaining the flexibility of neural architectures. Future work will focus on enhancing interpretability, expanding the diversity of training data, and generalizing the framework to a broader class of hydrogel chemistries and network structures. These developments have the potential to advance automated constitutive model discovery and accelerate the design of next-generation degradable materials.

REFERENCES

- [1] H. Holthusen, L. Lamm, T. Brepols, S. Reese, and E. Kuhl, “Theory and implementation of inelastic Constitutive Artificial Neural Networks,” *Computer Methods in Applied Mechanics and Engineering*, vol. 428, p. 117063, 2024. doi: 10.1016/j.cma.2024.117063.
- [2] Z. Pan and L. Brassart, “Constitutive modelling of hydrolytic degradation in hydrogels.” *Journal of the Mechanics and Physics of Solids*, vol. 165, p. 104902, 2022. doi: 10.1016/j.jmps.2022.104902.
- [3] R. Abi-Akl, E. Ledieu, T. N. Enke, O. X. Cordero, and T. Cohen, “Physics-based prediction of biopolymer degradation,” *Soft Matter*, vol. 15, pp. 4098–4108, 2019. doi: 10.1039/C9SM00262F.
- [4] M. Flaschel, P. Steinmann, L. De Lorenzis, and E. Kuhl, “Convex Neural Networks Learn Generalized Standard Material Models,” *Journal of the Mechanics and Physics of Solids*, vol. 200, p. 106103, 2025. doi: 10.1016/j.jmps.2025.106103.
- [5] K. Linka, S. R. St Pierre, and E. Kuhl, “Automated model discovery for human brain using Constitutive Artificial Neural Networks,” *Acta Biomaterialia*, vol. 160, pp. 134–151, 2023. doi: 10.1016/j.actbio.2023.01.055.